Finite-volume solution of one-dimensional shallow-water sensitivity equations

Vincent Guinot, Bernard Cappelaere, Carole Delenne

Finite-volume solution of one-dimensional shallow-water sensitivity equations
Résolution aux volumes finis des équations en sensibilité pour les écoulements à surface libre unidimensionnels

VINCENT GUINOT (IAHR Member), Professor, *HydroSciences Montpellier (HSM) UMR 5569 (CNRS, IRD, UM1, UM2)*, *Université Montpellier 2*, *CC MSE*, *34095 Montpellier Cedex 5, France*. *Tel +33 4 67 14 90 56; fax: +33 4 67 14 47 74; E-Mail: guinot@msem.univ-montp2.fr*

BERNARD CAPPELAERE, Research Engineer, *HydroSciences Montpellier (HSM) UMR 5569 (CNRS, IRD, UM1, UM2)*, *Université Montpellier 2*, *CC MSE*, *34095 Montpellier Cedex 5, France*. *Tel +33 4 67 14 90 17; fax: +33 4 67 14 47 74; E-Mail: cappelaere@msem.univ-montp2.fr*

CAROLE DELENNE, Lecturer, *HydroSciences Montpellier (HSM) UMR 5569 (CNRS, IRD, UM1, UM2)*, *Université Montpellier 2*, *CC MSE*, *34095 Montpellier Cedex 5, France*. *Tel +33 4 67 14 90 24; fax: +33 4 67 14 47 74; E-Mail: delenne@msem.univ-montp2.fr*

Abstract
Solving the Shallow-Water-Sensitivity Equations for discontinuous flows involves the discretization of a Dirac source term accounting for discontinuities. Failing to account for this source term usually results in solution instability, with empirical sensitivity solutions exhibiting artificial peaks in the neighbourhood of shocks. An extension of the Harten-Lax-van Leer approximate Riemann solver is presented that allows the one-dimensional shallow-water-sensitivity equations to be discretized more accurately than in previously published versions. A discretization of boundary conditions and source terms is also provided. The proposed discretization allows for discontinuities in both the hydraulic and sensitivity boundary conditions. Numerical experiments indicate the superiority of the proposed approach for sensitivity analysis over the classical, empirical approach if the flow solution is discontinuous. A numerical convergence analysis demonstrates that the numerical and analytical solutions converge.

RÉSUMÉ
La résolution numérique des équations en sensibilité pour les écoulements unidimensionnels à surface libre implique de discrétiser un terme source de type Dirac qui s'applique au niveau des discontinuités de l'écoulement. Négliger ce terme source conduit généralement à l'instabilité de la solution numérique. Ainsi, les sensibilités calculées par la méthode empirique présentent des pics artificiels au niveau des chocs. Cet article présente une extension du solveur approché Harten-Lax-van Leer conduisant à une résolution plus précise des équations en sensibilité pour les écoulements à surface libre que les versions précédemment publiées. On présente également la discrétisation des termes sources et des conditions aux limites en sensibilité. Les applications numériques indiquent que la méthode proposée apporte des améliorations importantes par rapport à l'approche empirique classique en présence de solutions discontinues. Une étude numérique montre la convergence de la solution numérique vers la solution analytique.

Keywords: Boundary condition, Finite volume, Free surface flow, Riemann solver, Sensitivity

1 Introduction

Sensitivity analysis is widely used in engineering problems (Helton et al. 2006), either in optimisation problems such as model calibration (White et al. 2003), flow or pollution control (Piasecki and Katopodes 1997, Sanders and Katopodes 1999), geometry optimization (Pironneau 1974), data assimilation (Gejadze and Copeland 2005), or experimental design (Atkinson and Donev 1992, Anderson et al. 2005), or in scenario analysis, such as uncertainty analysis (Maskey and Guinot 2003, Pappenberger et al. 2006). It is also used in reliability and risk analyses (Andrade Lima et al. 1998, Patil and Frey 2004). Model sensitivity analysis techniques may be divided into continuous approaches, whereby the governing equations are differentiated with respect to the parameter of interest and then solved numerically, and discrete approaches, whereby the governing equations are first solved numerically and then differentiated with respect to the parameter of interest. The latter approach is more suitable to the analysis of model response, where the transfer function between the model inputs and outputs is not known

exactly and therefore cannot be formulated mathematically. Discrete approaches (Griewank 2000, Kleiber et al. 1997) include code differentiation either manual or automatic (Elizondo et al. 2002), complex differentiation (Lyness and Moler 1967), or the so-called finite difference, or empirical approach, consisting in carrying out two simulations using slightly different values of the parameter of interest and computing the sensitivity as the ratio of the difference between the simulation results to the variation in the parameter.

Classical sensitivity analysis methods meet problems if the model output becomes discontinuous (Gunzburger 1999). This is the case when solving the Shallow-Water Equations (SWE) in the presence of hydraulic jumps or moving bores. The non-differentiable character of the flow solution yields locally infinite sensitivity values across discontinuities. This led Bardos and Pironneau (2002) to formulating sensitivity equations in the framework of the theory of distributions, thereby introducing sensitivity source terms in the form of Dirac functions across shocks. The need for a Dirac-type formulation of the sensitivity source term for scalar hyperbolic problems was acknowledged using a different reasoning in Guinot et al. (2007) and applied to design numerical methods for hyperbolic systems of conservation laws (Delenne et al. 2008, Guinot et al. 2009). The accurate discretization of this Dirac source term in the framework of shock-capturing numerical methods poses a number of problems and, although solutions are proposed by Delenne et al. (2008) and Guinot et al. (2007, 2009), they prove not to be entirely satisfactory in a number of cases (Guinot et al. 2009).

The purpose of this research is to present a finite volume-based numerical technique for the computation of the sensitivity of the solutions of the one-dimensional (1D) SWEs. The computation of the fluxes at internal points is presented, as well as the complete discretization of boundary conditions. The structure is as follows. In Section 2, the SWEs are presented, the derivation of the Shallow Water Sensitivity Equations (SWSEs) is outlined for the continuous case and the expressions of the sensitivity source term, initial and boundary conditions are derived. Section 3 is devoted to the detailed presentation of the numerical technique for discontinuous solutions, with a focus on the source term and boundary condition discretization. Application examples are provided in Section 4. Section 5 is devoted to concluding remarks.

2 Governing equations

2.1 *Sensitivity equations*

The one-dimensional SWEs can be written in vector form as

$$\frac{\partial \mathbf{U}}{\partial t} + \frac{\partial \mathbf{F}}{\partial x} = \mathbf{S} \tag{1}$$

where the conserved variable **U**, the flux vector **F** and the source term **S** are defined as

$$\mathbf{U} = \begin{bmatrix} h \\ q \end{bmatrix}, \mathbf{F} = \begin{bmatrix} q \\ q^2/h + gh^2/2 \end{bmatrix}, \ \mathbf{S} = \begin{bmatrix} 0 \\ gh(S_o - S_f) \end{bmatrix} \tag{2}$$

where g = gravitational acceleration, h = flow depth, q = unit discharge, S_o and S_f = bottom and friction slopes, respectively. In what follows, the friction slope is assumed to obey a classical Manning-Strickler law under the wide channel approximation for the sake of conciseness of the mathematical developments

$$S_f = n_M^2 |q| q h^{-10/3} = n_M^2 |u| u h^{-4/3} \tag{3}$$

where n_M = Manning's friction coefficient and $u = q/h$ = flow velocity.

In Eq. (1), the flux function **F** and the source term **S** may depend on several parameters, such as gravitational acceleration, friction coefficient n_M, or initial and/or boundary conditions. The sensitivity analysis is carried out using the so-called perturbation approach, that consists in studying the effect of a small perturbation in the parameter on the solution of the flow equations. This leads to the governing equations for the sensitivity, called sensitivity equations hereafter. As shown by Delenne et al. (2008), Guinot et al. (2007, 2009), SWSEs are given by

$$\frac{\partial \mathbf{s}}{\partial t} + \frac{\partial \mathbf{G}}{\partial x} = \mathbf{Q} + \mathbf{R} \tag{4}$$

with

$$\mathbf{s} = \begin{bmatrix} \eta \\ \theta \end{bmatrix} = \begin{bmatrix} \partial h / \partial \varphi \\ \partial q / \partial \varphi \end{bmatrix} \tag{5a}$$

$$\mathbf{G} = \frac{\partial \mathbf{F}}{\partial \mathbf{U}} \mathbf{s} = \begin{bmatrix} 0 & 1 \\ c^2 - u^2 & 2u \end{bmatrix} \mathbf{s} = \begin{bmatrix} \theta \\ (c^2 - u^2)\eta + 2u\theta \end{bmatrix} \tag{5b}$$

$$\mathbf{Q} = \frac{\partial \mathbf{S}}{\partial \mathbf{U}} \mathbf{s} + \frac{\partial \mathbf{S}}{\partial \varphi} \varepsilon - \frac{\partial}{\partial x} \left(\frac{\partial \mathbf{F}}{\partial \varphi} \varepsilon \right) \tag{5c}$$

$$\mathbf{R} = [\mathbf{s}] c_s - [\mathbf{G}] \tag{5d}$$

where $c = (gh)^{1/2}$, c_s = speed of discontinuities in the solution, φ = = parameter of sensitivity analysis and the square bracket operator [ ] denotes a jump in the quantity between brackets across a discontinuity. If the solution is constant on both sides of a discontinuity and $\varepsilon = 0$ across the discontinuity, Eq. (5d) simplifies to (Guinot et al. 2009)

$$\mathbf{R} = \frac{\partial c_s}{\partial \varphi} [\mathbf{U}] \tag{6}$$

Note that the source term **R** in Eq. (4) is nonzero only at points where **U** is discontinuous. Equations (4) to (6) are the conservation form of the SWSEs. Note that in Eq. (5c) the first term on the right-hand side is given by

$$\frac{\partial \mathbf{S}}{\partial \mathbf{U}} \mathbf{s} = \begin{bmatrix} 0 \\ (S_o + 7/3 S_f) g \eta - 2 g n_M^2 |q| h^{-7/3} \theta \end{bmatrix} \tag{7}$$

The only term in Eq. (4) that depends on the nature of φ is the source term **Q** defined in Eq. (5c). In the following, the expression of **Q** is provided for the sensitivity to the friction coefficient and the initial conditions.

An expression for **Q** is derived for the particular case where the parameter φ is Manning's friction coefficient n_M. Since **F** is not a function of n_M, Eq. (5c) simplifies to

$$\mathbf{Q} = \frac{\partial \mathbf{S}}{\partial \mathbf{U}} \mathbf{s} + \frac{\partial \mathbf{S}}{\partial \varphi} \varepsilon = \begin{bmatrix} 0 \\ \left(S_o + \dfrac{7 S_f}{3} \right) g \eta - 2 g n_M^2 |q| h^{-7/3} \theta - 2 g h \dfrac{S_f}{n_M} \varepsilon \end{bmatrix} \tag{8}$$

where $\varepsilon = 0$ in regions where the friction coefficient remains constant and $\varepsilon = 1$ in regions where the friction coefficient is the parameter of interest in the sensitivity analysis.

2.2 *Sensitivity to initial conditions*

The sensitivity to the initial conditions of a flow problem is studied by defining φ as one of the flow variables (h, q, or u) at $t = 0$. Since **F** and **S** at any time $t > 0$ do not depend on the value of **U** at $t = 0$, the expression of **Q** reduces to

$$\mathbf{Q} = \frac{\partial \mathbf{S}}{\partial \mathbf{U}}\mathbf{s} = \begin{bmatrix} 0 \\ \left(S_o + \dfrac{7S_f}{3}\right)g\eta - 2gn_M^2|q|h^{-7/3}\theta \end{bmatrix} \tag{9}$$

and the initial condition for the SWSE (6) is given by

$$\mathbf{s}(x,0) = \begin{bmatrix} \varepsilon_h \\ \varepsilon_q \end{bmatrix} \tag{10}$$

where ε_h and ε_q = perturbation indicators for the initial flow depth $h(x, 0)$ and unit discharge $q(x, 0)$.

Assume for instance that the dambreak problem (Stoker 1957) is to be solved and that the purpose of the analysis is to study the sensitivity of the flow solution to the flow depth h_L on the left-hand side of the dam. Then the perturbation indicators ε_h and ε_q in Eq. (10) must be defined as

$$\varepsilon_h(x) = \begin{cases} 1 & \text{for } x < x_0 \\ 0 & \text{for } x > x_0 \end{cases} \tag{11a}$$

$$\varepsilon_q(x) = 0 \qquad \forall x \tag{11b}$$

where x_0 = dam location.

2.3 *Boundary conditions*

Boundary conditions for a flow are relationships in the form

$$f(h_b, q_b, \varphi, t) = 0 \tag{12}$$

where subscript b denotes the value of the flow variables at the boundary. As shown by Cunge et al. (1980), as many boundary conditions must be supplied at a given boundary as there are characteristics $\mathrm{d}x/\mathrm{d}t = u \pm c$ entering the domain. It stems from Eq. (5b) that the Jacobian matrix $\partial\mathbf{G}/\partial\mathbf{s}$ for the sensitivity problem is identical to the Jacobian matrix $\partial\mathbf{F}/\partial\mathbf{U}$ for the original flow problem. Consequently, the characteristics of the sensitivity problem are identical to the characteristics of the flow problem and the sensitivity problem requires as many boundary conditions as the original flow problem.

Two situations may occur:

(1) The sensitivity analysis is carried out with respect to the initial conditions or a hydrodynamic parameter. Then, the boundary conditions are not influenced by the value of φ and differentiating Eq. (12) with respect to φ yields

$$\frac{\partial f}{\partial h_b}\eta_b + \frac{\partial f}{\partial q_b}\theta_b = 0, \tag{13}$$

(2) The sensitivity analysis is carried out with respect to the boundary condition. This is the case if the numerical value of the boundary condition to be prescribed is not known with certainty, or measured with a certain imprecision. Differentiating Eq. (12) leads to

$$\frac{\partial f}{\partial h_b}\eta_b + \frac{\partial f}{\partial q_b}\theta_b + \frac{\partial f}{\partial \varphi} = 0 \tag{14}$$

Consider for instance that a known flow depth $h_b(t)$ is to be prescribed at a boundary. Eq. (12) becomes

$$h - h_b = 0 \tag{15}$$

Applying Eq. (14) with $\varphi = h_b$ yields the following sensitivity boundary condition

$$\eta_b = 1 \tag{16}$$

For a prescribed unit discharge q_b, the sensitivity boundary condition is

$$\theta_b = 1 \tag{17}$$

3 Numerical technique

3.1 *Finite volume discretization*

The flow and sensitivity equations are discretized using an explicit finite volume formulation (Guinot 2009)

$$\mathbf{U}_i^{n+1} = \mathbf{U}_i^n + \frac{\Delta t}{\Delta x_i}(\mathbf{F}_{i-1/2}^n - \mathbf{F}_{i+1/2}^n) + \Delta t \mathbf{S}_i^n \tag{18a}$$

$$\mathbf{s}_i^{n+1} = \mathbf{s}_i^n + \frac{\Delta t}{\Delta x_i}(\mathbf{G}_{i-1/2}^n - \mathbf{G}_{i+1/2}^n) + \Delta t \mathbf{Q}_i^n \tag{18b}$$

where $\mathbf{U}_i^n$ and $\mathbf{s}_i^n$ denote, respectively, the average value of **U** and **s** over the cell i at time level n, $\mathbf{F}_{i-1/2}^n$ and $\mathbf{G}_{i-1/2}^n$ = values of **F** and **G** at the interface $i - 1/2$ between cells $i - 1$ and i, $\mathbf{S}_i^n$ and $\mathbf{Q}_i^n$ = average values of **S** and **Q** over the cell i, Δt = computational time step and Δx_i = width of cell i. The hyperbolic part of the equation and the source term are treated in separate subsections hereafter.

3.2 *Flux calculation*

The fluxes are computed using the original Harten-Lax-van Leer (HLL) Riemann solver for the flow problem and a modified HLL solver for the sensitivity problem. In the HLL Riemann solver (Harten et al. 1983, Ying and Wang 2008) the two waves separating the intermediate region of constant state from the left (subscript L) and right (subscript R) states of the Riemann problem are assumed to be discontinuities. Writing the balance equations across the discontinuities leads to

$$\mathbf{F}_{i-1/2}^n = \frac{\lambda_{\max}\mathbf{F}_L - \lambda_{\min}\mathbf{F}_R - \lambda_{\min}\lambda_{\max}(\mathbf{U}_L - \mathbf{U}_R)}{\lambda_{\max} - \lambda_{\min}} \tag{19a}$$

$$\lambda_{\min} = \min(\lambda^-, 0) \tag{19b}$$

$$\lambda_{\max} = \max(\lambda^+, 0) \tag{19c}$$

$$\mathbf{U}_* = \frac{-\lambda^-\mathbf{U}_L + \lambda^+\mathbf{U}_R + \mathbf{F}_L - \mathbf{F}_R}{\lambda^+ - \lambda^-} \tag{19d}$$

where subscript * denotes the value of the variable in the intermediate region of constant state. In the first component of Eq. (19a), the free surface elevations z_L and z_R are used instead of the original conserved variables h_L and h_R for well-balancing of the flux and

topographical source term (Nujic 1995). In the present applications, λ^- and λ^+ are computed as (Davis 1988)

$$\lambda^- = \min(u_L - c_L, u_R - c_R) \tag{20a}$$

$$\lambda^+ = \max(u_L + c_L, u_R + c_R) \tag{20b}$$

The sensitivity flux **G** is obtained by extending Eq. (19a) to the sensitivity balance

$$\mathbf{G}^n_{i-1/2} = \frac{\lambda_{\max}\mathbf{G}_L - \lambda_{\min}\mathbf{G}_R - \lambda_{\min}\lambda_{\max}(\mathbf{s}_L - \mathbf{s}_R)}{\lambda_{\max} - \lambda_{\min}} \tag{21}$$

Since the Eigenvalues of the Jacobian matrices $\partial\mathbf{F}/\partial\mathbf{U}$ and $\partial\mathbf{G}/\partial\mathbf{s}$ are identical, the stability constraint is the same for the flow and sensitivity problems. The maximum permissible computational time step $\Delta t_{\max}$ is such that the Courant-Friedrichs-Lewy (CFL) number associated to the faster of the waves $u - c$ and $u + c$ is smaller than unity, i.e.

$$\Delta t_{\max} = \min_i \frac{\Delta x_i}{\left|u_i^n\right| + c_i^n} \tag{22}$$

Note that the explicit discretization of the friction and sensitivity source terms should be expected to introduce an additional stability constraint: The computational time step should be such that the friction term does not induce a change in the flow direction over a computational time step. However, in all practical applications encountered so far, the hyperbolic part of the equations has always been seen to be the predominant factor in time step limitation, and Eq. (22) proves to be a sufficient criterion in practice.

3.3 *Source term calculation*

The source term **S** in Eq. (18a) is computed as

$$\mathbf{S}_i^n = \mathbf{S}_{f_i}^{\ n} + \mathbf{S}_{g_i}^{\ n} \tag{23}$$

where $\mathbf{S}_f$ and $\mathbf{S}_g$ = parts of **S** originating from frictional and geometric terms, respectively. $\mathbf{S}_f$ is computed using an explicit, cell-centred formulation

$$\mathbf{S}_{f_i}^{\ n} = \begin{bmatrix} 0 \\ -gn_M^2\left|u_i^n\right|u_i^n h_i^{n^{-1/3}} \end{bmatrix} \tag{24}$$

while the geometric source term is discretized using a classical source term upwinding procedure (Vazquez-Cendon 1999)

$$\mathbf{S}_{g_i}^{\ n} = \begin{bmatrix} 0 \\ ghS_o \end{bmatrix}_{i,L}^n + \begin{bmatrix} 0 \\ ghS_o \end{bmatrix}_{i,R}^n \tag{25}$$

where the subscripts L and R denote the respective contributions of the left and right interface of cell i to the total source term. The contributions of the interface i–1/2 to the cells i – 1 and i are given by

$$(ghS_o)_{i,L}^n = \frac{-\lambda_{\min}}{\lambda_{\max} - \lambda_{\min}} g \frac{h_{i-1}^n + h_i^n}{2}(z_{b\,i-1} - z_{b\,i}) \tag{26a}$$

$$(ghS_o)_{i-1,R}^n = \frac{\lambda_{\max}}{\lambda_{\max} - \lambda_{\min}} g \frac{h_{i-1}^n + h_i^n}{2}(z_{b\,i-1} - z_{b\,i}) \tag{26b}$$

where z_b = bottom (subscript b) elevation.

The source term **Q** is split into the three parts

$$\mathbf{Q}_i^n = \mathbf{Q}_{f_i}^{\ n} + \mathbf{Q}_{g_i}^{\ n} + \mathbf{R}_i^n \tag{27}$$

where $\mathbf{Q}_f$ and $\mathbf{Q}_g$ are respectively the parts of the source term due to friction and the variations in the friction coefficient perturbation indicator ε, and to the geometric terms, and **R** = source term arising from the possible presence of shocks in the solution. $\mathbf{Q}_f$ and $\mathbf{Q}_g$ are discretized using the classical cell-centred and source term upwinding approach

$$\mathbf{Q}_{f_i}^{\ n} = \left[\begin{array}{c} 0 \\ \dfrac{7S_f}{3} g\eta - 2gn_M^2 |q| h^{-7/3}\theta - 2gh \dfrac{S_f}{n_M} \varepsilon_{n_M} \end{array} \right]_i^n \tag{28a}$$

$$\mathbf{Q}_{g_i}^{\ n} = \left[\begin{array}{c} 0 \\ S_o g\eta \end{array} \right]_{i,L}^n + \left[\begin{array}{c} 0 \\ S_o g\eta \end{array} \right]_{i,R}^n \tag{28b}$$

with

$$(S_o g\eta)_{i,L}^n = \frac{-\lambda_{\min}}{\lambda_{\max} - \lambda_{\min}} g \frac{\eta_{i-1}^n + \eta_i^n}{2} (z_{bi-1} - z_{bi}) \tag{29a}$$

$$(S_o g\eta)_{i-1,R}^n = \frac{\lambda_{\max}}{\lambda_{\max} - \lambda_{\min}} g \frac{\eta_{i-1}^n + \eta_i^n}{2} (z_{bi-1} - z_{bi}) \tag{29b}$$

The point source term **R** is split into two contributions: the contribution $\mathbf{R}^-$ of wave λ^- and the contribution $\mathbf{R}^+$ of wave λ^+. $\mathbf{R}^-$ and $\mathbf{R}^+$ are discretized as (Guinot 2009)

$$\mathbf{R}^- = \begin{cases} \dfrac{(u_L + c_L/2)\eta_L - \theta_L}{h_L} (\mathbf{U}_L - \mathbf{U}_*) & \text{if } u_L - c_L < u_R - c_R \\ \dfrac{(u_R + c_R/2)\eta_R - \theta_R}{h_R} (\mathbf{U}_L - \mathbf{U}_*) & \text{if } u_L - c_L > u_R - c_R \end{cases} \tag{30a}$$

$$\mathbf{R}^+ = \begin{cases} \dfrac{(u_L - c_L/2)\eta_L - \theta_L}{h_L} (\mathbf{U}_* - \mathbf{U}_R) & \text{if } u_L + c_L > u_R + c_R \\ \dfrac{(u_R - c_R/2)\eta_R - \theta_R}{h_R} (\mathbf{U}_* - \mathbf{U}_R) & \text{if } u_L + c_L < u_R + c_R \end{cases} \tag{30b}$$

3.4 *Shock detection*

The source term **R** is nonzero and must be accounted for in Eq. (27) only if one of the waves λ^-, λ^+ is a shock. Consequently, a shock detection procedure must be implemented to identify the interfaces at which the Riemann problem gives rise to shock waves. A shock is detected for wave λ^- if the following conditions are satisfied (Delenne et al. 2008, Guinot 2009, Guinot et al. 2009)

$$u_L - c_L > u_* - c_* \tag{31a}$$

$$u_L + c_L > u_* + c_* \tag{31b}$$

while a shock is detected for wave λ^+ if

$$u_* - c_* > u_R - c_R \tag{32a}$$

$$u_* + c_* > u_R + c_R \tag{32b}$$

3.5 *Discretization of boundary conditions*

Three types of boundary conditions are considered hereafter, related to a prescribed discharge, flow depth, or stage-discharge relationship. For the sake of conciseness, only the left-hand boundary of the domain is considered, the transposition to a right-hand boundary being straightforward. Only subcritical flow is considered hereafter, the supercritical case being straightforward.

(1) *Prescribed flow depth* Assume that the flow depth h_b is to be prescribed at the left-hand boundary. Then, the flow depth and the sensitivity at the left-hand interface ½ of the computational cell 1 are given by

$$h_{1/2}^n = h_b \tag{33a}$$

$$\eta_{1/2}^n = \eta_b \tag{33b}$$

with $\eta_b = 0$ or 1, depending on the purpose of the sensitivity analysis (see 2.4). The values of q and θ at the boundary are computed by considering, as in Eq. (24), that the boundary states $[h_b, q_b]^T$ and $[\eta_b, \theta_b]^T$ are separated from the inside of the computational domain by a discontinuity moving at speed $\lambda^+ = u_1^n + c_1^n$. Then, one has

$$q_{1/2}^n = q_1^n + (h_b - h_1^n)\lambda^+ \tag{34a}$$

$$\theta_{1/2}^n = \theta_1^n + (\eta_b - \eta_1^n)\lambda^+ \tag{34b}$$

The flow depth $h_{1/2}^n$ and the unit discharge $q_{1/2}^n$ being entirely determined at the interface 1/2, the calculation of the momentum flux $q^2/h + gh^2/2$ is straightforward. The second component of **G** is computed using the known values of h, q, η and θ at the boundary.

(2) *Prescribed unit discharge* The boundary conditions are

$$q_{1/2}^n = q_b \tag{35a}$$

$$\theta_{1/2}^n = \theta_b \tag{35b}$$

Following (1) yields directly the second flux component for the flow variable and sensitivity

$$(F_2)_{1/2}^n = (F_2)_1^n + (q_b - q_1^n)\lambda^+ \tag{36a}$$

$$(G_2)_{1/2}^n = (G_2)_1^n + (\theta_b - \theta_1^n)\lambda^+ \tag{36b}$$

(3) *Prescribed stage-discharge relationship* For a known, nonlinear relationship between the flow depth and the unit discharge, it is more convenient to rewrite Eq. (12) in the form of a relationship between flow velocity u and wave celerity in still water c as

$$f(u_b, c_b, \varphi) = 0 \tag{37a}$$

$$\frac{\partial f}{\partial u_b}\upsilon_b + \frac{\partial f}{\partial c_b}\chi_b + \frac{\partial f}{\partial \varphi} = 0 \tag{37b}$$

where χ and υ are the sensitivity of c and u, respectively. This set of equations is complemented by the Riemann invariants $u - 2c$ and $\upsilon - 2\chi$ for flow and sensitivity, respectively,

$$u_{1/2}^n - 2c_{1/2}^n = u_1^n - 2c_1^n \tag{38a}$$

$$\upsilon_{1/2}^n - 2\chi_{1/2}^n = \upsilon_1^n - 2\chi_1^n \tag{38b}$$

Equations (37) and (38) can be solved uniquely for u, c and the sensitivities υ and χ.

4 Computational examples

4.1 *Dambreak problem*

The dambreak problem is a Riemann problem, i.e. an initial value problem defined as (Stoker 1957)

$$h(x,0) = \begin{cases} h_L & \text{for } x < x_0 \\ h_R & \text{for } x > x_0 \end{cases} \tag{39a}$$

$$q(x,0) = 0 \tag{39b}$$

where $h_L > h_R$ if the reservoir is located on the left-hand side of the dam. The purpose is to study the sensitivity of the flow solution to the initial flow depth h_L in the reservoir. As indicated in 2.3, the initial conditions for the sensitivity problem are given by

$$\eta(x,0) = \begin{cases} 1 & \text{for } x < x_0 \\ 0 & \text{for } x > x_0 \end{cases} \tag{40a}$$

$$\theta(x,0) = 0 \tag{40b}$$

The parameters of the test case are stated in Table 1.

Table 1 Dambreak problem, parameters of test case

Symbol	Meaning	Value
g	Gravitational acceleration	9.81 m s^{-2}
L	Length of simulation domain	1000 m
h_L	Flow depth on left-hand side of initial discontinuity	10 m
h_R	Flow depth on right-hand side of initial discontinuity	1 m
x_0	Abscissa of initial discontinuity	500 m
Δt	Computational time step	$\Delta t_{\max}$ Eq. (29)
Δx	Cell width	1 m
η_L	Depth sensitivity on left-hand side of initial discontinuity	1
η_R	Depth sensitivity on right-hand side of initial discontinuity	0

The computational time step is the maximum permissible time step given by Eq. (22). The numerical and analytical solutions are compared at $t = 30$ s (Fig. 1). A detailed derivation of the analytical sensitivity solution is given by Guinot et al. (2009).

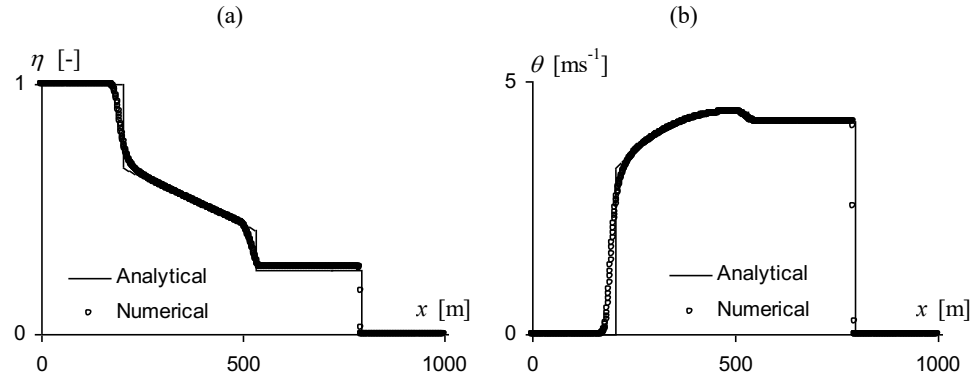

Figure 1 Dambreak problem, analytical and numerical sensitivity solutions. Sensitivity of (a) flow depth, (b) unit discharge

A striking feature of the analytical solution is the discontinuous character of the sensitivity across the boundaries of rarefaction waves. Within the rarefaction wave, η is a linear function of x/t. The numerical solution obtained using the proposed solver is seen in Fig. 1 to allow for a correct location of the discontinuities in the sensitivity profiles. The shock is described using only two cells in space, while inevitable numerical diffusion occurs across the boundaries of the rarefaction wave. Figure 2 illustrates the invalidity of the empirical approach in the neighbourhood of shocks. In Fig. 2 (a) and (c), an artificial overshoot is clearly visible across the shock. Its magnitude exceeds the initial magnitude of the sensitivity by a factor of 30 (Fig. 2 b and d).

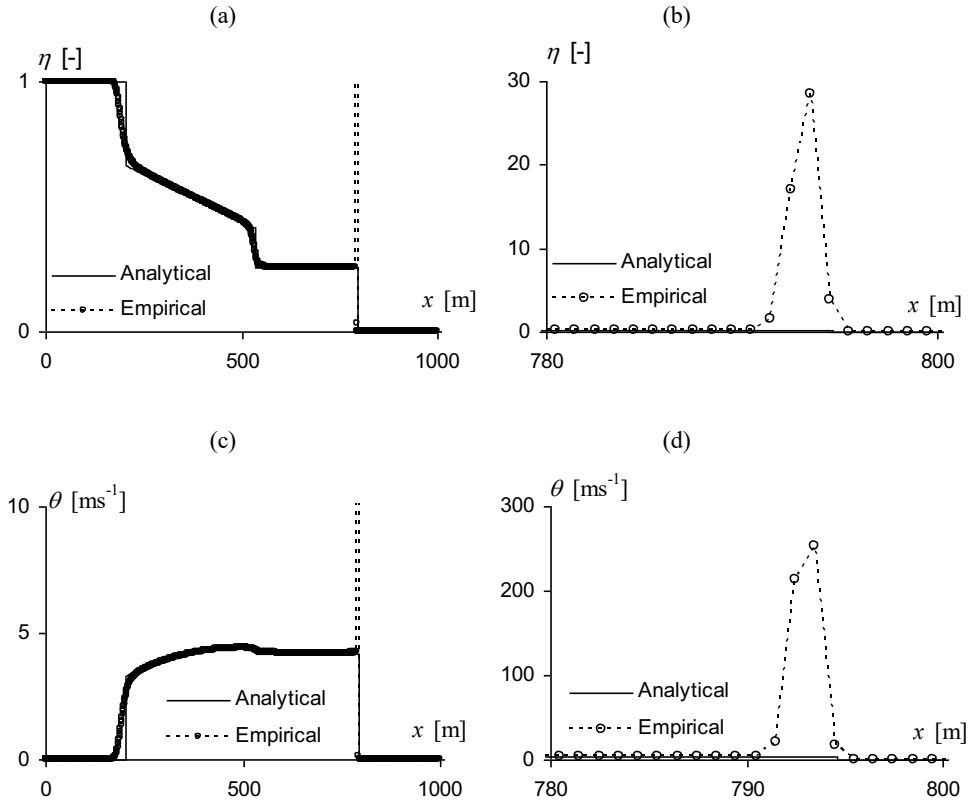

Figure 2 Dambreak problem, analytical and empirical sensitivity solutions. (a) Flow depth sensitivity profile, (b) zoomed view over interval [780 m, 800 m], (c) unit discharge sensitivity profile, (d) zoomed view over interval [780 m, 800 m]

4.2 *Bore propagation into a frictionless channel*

The purpose of this test is to assess the accuracy of the proposed discretization for the sensitivity boundary conditions in presence of discontinuous solutions. A convergence study was also carried out. Consider a horizontal, frictionless channel where the water is initially immobile, with a constant initial depth h_0. At $t = 0$, the unit discharge at the left-hand channel end ($x = 0$) changes instantaneously from 0 to a constant value q_b. A bore appears and propagates into the channel at constant speed c_s. Writing the jump relationships across the bore leads to

$$q_b = (h_b - h_0)c_s \tag{41a}$$

$$\frac{q_b^2}{h_b} + \frac{g}{2}(h_b^2 - h_0^2) = q_b c_s \tag{41b}$$

where h_b = boundary flow depth. Equations (41) are solved uniquely for h_b and c_s. Since the purpose is to study the solution sensitivity to q_b, the parameter φ in the sensitivity analysis is defined as $\varphi = q_b$ and the sensitivity boundary condition is given by Eq. (17).

The jump relationships for the sensitivity are obtained by differentiating Eqs. (41) with respect to q_b, using Eq. (17) for θ_b, and noticing that the initial flow depth sensitivity $\eta_0 = 0$

$$\eta_b c_s + (h_b - h_0)\frac{\partial c_s}{\partial q_b} = 1 \tag{42a}$$

$$2u_b - u_b^2\eta_b + gh_b\eta_b = c_s + q_b \frac{\partial c_s}{\partial q_b} \tag{42b}$$

The set of parameters used for this application example are given in Table 2. Solving Eqs. (41) and (42) yields $c_s = 3.75$ m s^{-1}, $h_b = 1.27$ m, $h_b = 0.23$ s m^{-1}, $\partial c_s/\partial q_b = 0.53$ m^{-1}. Figure 3 compares the numerical sensitivity profiles at $t = 20$ s to the analytical and empirical solutions.

Table 2 Problem parameters for bore propagation into a frictionless channel

Symbol	Meaning	Value
g	Gravitational acceleration	9.81 m s^{-2}
h_0	Initial flow depth	1 m
L	Length of channel	100 m
q_b	Unit discharge at upstream boundary	1 m^2 s^{-1}
Δt	Computational time step	$\Delta t_{\max}$ Eq. (29)
Δx	Cell width	1 m
η_b	Downstream depth sensitivity	0
θ_b	Upstream discharge sensitivity	1

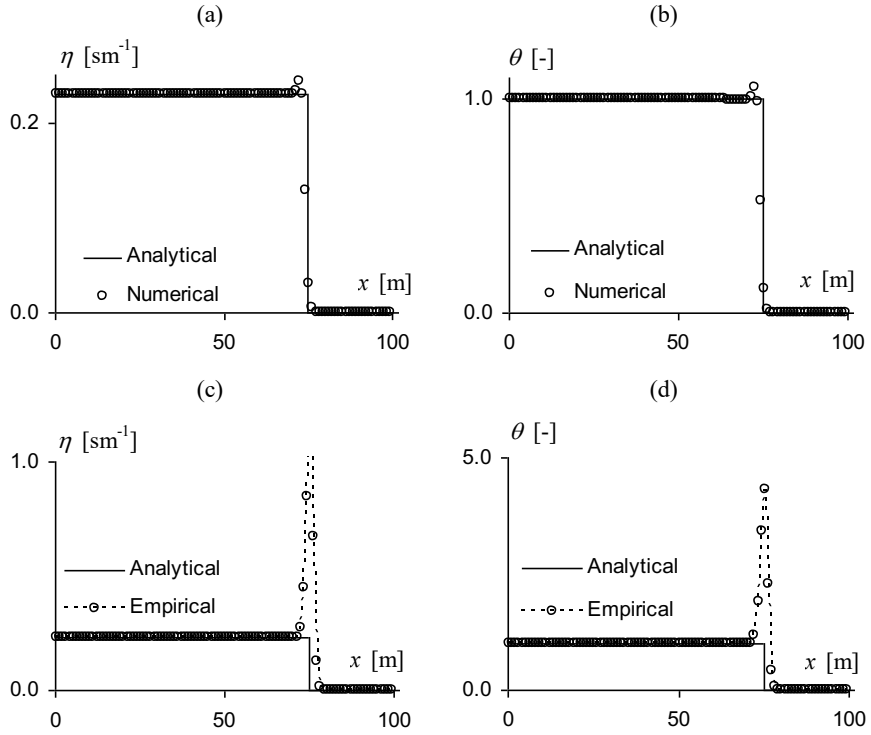

Figure 3 Bore propagation into a frictionless channel. Analytical and numerical sensitivity profiles for (a) flow depth, (b) unit discharge. Analytical and empirical sensitivity profiles for (c) flow depth, (d) unit discharge

The empirical sensitivity profiles are obtained from the difference between two flow simulations using slightly different values of q_b (here 0.01 m^{2}s^{-1}). Except for a small overshooting in the neighbourhood of the shock, the numerical sensitivity profile agrees well with the analytical solution and the propagation speed of the sensitivity discontinuity is well-reproduced. It should be stressed that the amplitude of the overshooting in the

numerical solution remains much smaller than the artificial peak in the empirical sensitivity profiles shown in Fig. 3.

Nevertheless, the presence of overshooting near the front may lead to question the accuracy of the method in the presence of steep transients arising from model boundaries. The accuracy of the method is investigated using a convergence analysis. The variations of the L1– and L2–norms of the difference between the numerical and analytical solutions with the cell width Δx are shown in Fig. 4. The Lp-Norm (p = 1, 2) is defined as

$$\mathrm{L}p = \left\{ \sum_i \left[U_i^n - U(x_i, t_n) \right]^p \Delta x_i \right\}^{1/p} \tag{43}$$

where U_i^n and $U(x_i, t_n)$ = numerical and analytical solutions at x_i at time t_n, respectively.

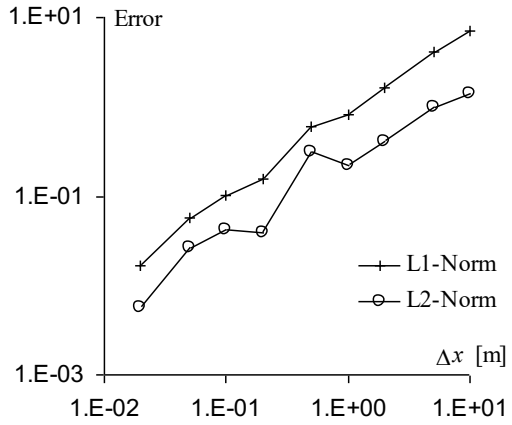

Figure 4 Bore propagation into a frictionless channel, with L1– and L2–Norms of the error in η as functions of cell size

As illustrated in Fig. 4, both the L1– and L2–Norms of the error decrease with Δx, indicating that the numerical solution converges to the analytical solution. The slopes of the two curves on the logarithmic graph is approximately equal to unity. For a continuous and differentiable solution, the slope of the L2–curve should be expected to be nearly twice as much as that of the L1–curve. The almost identical slopes for both norms indicate that most of the error is concentrated around the discontinuity and that the error is proportional to cell size, thus indicating that the smearing of the front and the small overshoot in the numerical solution remain confined to the same number of cells, regardless of cell width.

Note that a complete convergence study of the proposed numerical technique should also include an analysis of numerical convergence for unsteady sensitivity solutions in the presence of friction. However, analytical sensitivity solutions for such problems are not yet available. Also note that the present convergence study was carried out for a first-order reconstruction of the flow and sensitivity variables. The convergence analysis should be extended to higher-order numerical techniques using classical (Savic and Holly 1993) or faster, higher-order reconstruction techniques such as the MUSCL-EVR approach (Soares-Frazão and Guinot 2007).

5 Conclusions

A finite volume-based numerical technique has been presented for the direct solution of the one-dimensional shallow-water sensitivity equations in the presence of discontinuous solutions. Discontinuous flow solutions yield an increased complexity in the solution of the sensitivity problem because of the presence of a Dirac-type source term across shocks in the governing sensitivity equations. Compared to classical approaches such as the finite difference approach, the proposed method allows numerical artefacts including sensitivity peaks or infinite sensitivity values to be eliminated at discontinuities. The discretization of boundary conditions is shown to be robust, even in the presence of shocks and in the absence of the damping effect induced by friction. Although small sensitivity wiggles can be observed near shocks propagating from model boundaries, the numerical solution is demonstrated to converge to the analytical solution.

Acknowledgements

This work was supported by Research Contract ANR-05-PGCU-004, “RIVES” funded by the French Agence Nationale de la Recherche (ANR) / National Research Agency. The contribution and support of the following partners is gratefully acknowledged: Cemagref, CETE Méditerranée, CETMEF, LMFA UMR 5509 (CNRS, ECL, INSA Lyon, UCB), INSAVALOR, LCPC, LRPC Bordeaux, LRPC Clermont-Ferrand, Sogreah, URGC (INSA Lyon), UTC.

Notation

c = Wave propagation speed
$\mathbf{F}$ = Flux vector for flow problem
$\mathbf{G}$ = Flux vector for sensitivity problem
f = Mathematical function for boundary conditions
g = Gravitational acceleration
h = Flow depth
n_M = Manning’s friction coefficient
$\mathbf{Q}$ = Source term for sensitivity problem
$\mathbf{R}$ = Dirac source term
q = Unit discharge
$\mathbf{S}$ = Source term for flow problem
$\mathbf{s}$ = Sensitivity vector
S_o = Bottom slope
S_f = Friction slope
t = Time
$\mathbf{U}$ = Conserved flow variable vector
u = Flow velocity
x = Space coordinate
x_0 = Location of initial discontinuity

Greek Symbols

χ = Sensitivity of c
Δt = Computational time step
Δx = Cell width

ε = Perturbation indicator
η = Flow depth sensitivity
φ = Parameter in sensitivity analysis
θ = Unit discharge sensitivity
υ = Flow velocity sensitivity

Superscripts
n = Value at time level n
– = Variable associated with wave $u - c$
+ = Variable associated with wave $u + c$

Subscripts
b = Value at boundary
f = Contribution of friction to source term
g = Contribution of geometry to source term
i = Average value over cell i
i, L = Left-hand interface of cell i (interface $i - ½$)
i, R = Right-hand interface of cell i (interface $i + ½$)
L = Left state of Riemann problem
max = Maximum permissible value
R = Right state of Riemann problem
* = Variable in intermediate region of constant state

References

Anderson, M.L., Bangerth, W., Carey, G.F. (2005). Analysis of parameter sensitivity and experimental design for a class of nonlinear partial differential equations. *Intl. J. Num. Meth. Fluids* 48, 583-605.

Andrade Lima, F.R., Gandini, A., Blanco, A., Lira, C.A.B.O, Maciel, E.S.G., Alvim, A.C.M., Silva, F.C., Melo, P.F.F., França, W.F.L., Baliño, J.L., Larreteguy, A.E., Lorenzo, A. (1998). Recent advances in perturbative methods applied to nuclear engineering problems. *Progress in Nuclear Energy* 33(1-2), 23-97.

Atkinson, A.C., Donev, A.N. (1992). *Optimum experimental design.* Clarendon Press, Oxford UK.

Bardos, C., Pironneau, O. (2002). A formalism for the differentiation of conservation laws. *Comptes Rendus de l'Académie des Sciences* I 335, 839-845.

Cunge, J.A., Holly, F.M. Jr., Verwey, A. (1980). *Practical aspects of river computational hydraulics*. Pitman, London.

Davis, S.F. (1988). Simplified second-order Godunov-type methods. *SIAM Journal Scientific and Statistical Computing* 9, 455-473.

Delenne, C., Guinot, V., Cappelaere, B. (2008). Direct sensitivity computation for the Saint Venant equations with hydraulic jumps. *Comptes Rendus de Mécanique* 336, 766-771.

Elizondo, D., Cappelaere, B., Faure, C. (2002). Automatic versus manual model differentiation to compute sensitivities and solve non-linear inverse problems. *Computers and Geosciences* 28(3), 309-326.

Gejadze, I.Y., Copeland, G.J.M. (2005) Adjoint sensitivity analysis for fluid flow with free surface. *Intl. J. Num. Meth. Fluids*, 47 1027-1034.

Griewank, A. (2000). *Evaluating derivatives: Principles and techniques of algorithmic differentiation*. SIAM, Philadelphia PA.

Guinot, V. (2009). Upwind finite volume solution of sensitivity equations for hyperbolic systems of conservation laws with discontinuous solutions. *Computers & Fluids*, doi:10.1016/j.compfluid.2009.03.002.

Guinot, V., Delenne, C., Cappelaere, B. (2009). An approximate Riemann solver for sensitivity equations with discontinuous solutions. *Adv. Water Res.* 32, 61-77.

Guinot, V., Leménager, M., Cappelaere, B. (2007). Sensitivity equations for hyperbolic conservation law-based flow models. *Adv. Water Res.* 30, 1943-1961.

Gunzburger, M.D. (1999). Sensitivities, adjoints and flow optimization. *Intl. J. Num. Meth. Fluids* 3, 53-78.

Harten, A., Lax, P.D., van Leer, B. (1983). On upstream differencing and Godunov-type schemes for hyperbolic conservation laws. *J. Comp. Physics* 50, 235-269.

Helton, J.C., Cooke, R.M., McKay, M.D., Saltelli, A. (2006). Sensitivity analysis of model output: SAMO 2004. *Reliability Engineering and System Safety* 91, 1105-1108.

Kleiber, M., Antunez, H., Hien, T.D., Kowalczyk, P. (1997). *Parameter sensitivity in nonlinear mechanics*. Wiley, New York.

Lyness, J.N., Moler, C.B. (1967). Numerical differentiation of analytic functions. *SIAM J. Num. Analysis* 4(2), 202-210.

Maskey, S., Guinot, V. (2003). Improved first-order second moment method for uncertainty estimation in flood forecasting. *Hydrological Sci. J.* 48, 183-196.

Nujic, M. (1995). Efficient implementation of non-oscillatory schemes for the computation of free surface flows. *J. Hydraulic Res.* 33(1), 101-111.

Pappenberger, F., Matgen, P., Beven, K.J., Henry, J.-B., Pfister, L., Fraipont de, P. (2006). Influence of uncertain boundary conditions and model structure on flood inundation predictions. *Adv. Water Res.* 29, 1430-1449.

Patil, S.R., Frey, H.C. (2004). Comparison of sensitivity analysis methods based on applications to a food safety risk assessment model. *Risk Analysis* 24(3), 573-585.

Piasecki, M., Katopodes, N.D. (1997). Control of contaminant releases in rivers 1: Adjoint sensitivity analysis. *J. Hydraulic Engng*. 123(6), 486-492.

Pironneau, O. (1974). On optimum design in fluid mechanics. *J. Fluid Mech.* 64, 97-110.

Savic, L., Holly, F.M. Jr. (1993). Dambreak flood waves computed by modified Godunov method. *J. Hydraulic Res.* 31(2), 187-204.

Sanders, B.F., Katopodes, N.D. (1999). Control of canal flow by adjoint sensitivity method. *J. Irr. Drainage Engng*. 125(5), 287-297.

Soares-Frazão, S., Guinot, V. (2007). An eigenvector-based reconstruction scheme for the shallow-water equations on two-dimensional unstructured meshes. *Intl. J. Num. Meth. Fluids* 53, 23-55.

Stoker, J.J. (1957). *Water Waves*, Interscience, Wiley, New York.

Vazquez-Cendon, M.E. (1999). Improved treatment of source terms in upwind schemes for the shallow water equations in channels with irregular geometry. *J. Comp. Physics* 148(2), 497-526.

White, L.W., Vieux, B., Armand, D., LeDimet, F.X. (2003). Estimation of optimal parameters for a surface hydrology model. *Adv. Water Res.* 26(3), 337-348.

Ying, X, Wang, S.S.Y. (2008). Improved implementation of the HLL approximate Riemann solver for one-dimensional open channel flows, *J. Hydraulic Res.* 46(1), 21-34.